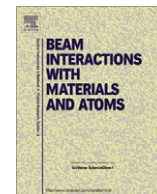




Contents lists available at SciVerse ScienceDirect

Nuclear Instruments and Methods in Physics Research B

journal homepage: www.elsevier.com/locate/nimb

High-sensitivity isobar-free AMS measurements and reference materials for ^{55}Fe , ^{68}Ge and ^{202}gPb

A. Wallner^{a,b,c,*}, M. Bichler^d, K. Buczak^a, D. Fink^b, O. Forstner^a, R. Golser^a, M.A.C. Hotchkis^b, A. Klix^e, A. Krasa^f, W. Kutschera^a, C. Lederer^a, A. Plompen^f, A. Priller^a, D. Schumann^g, V. Semkova^h, P. Steier^a

^a VERA Laboratory, Faculty of Physics, University of Vienna, Währinger Strasse 17, A-1090, Austria

^b Australian Nuclear Science and Technology Organisation (ANSTO), Lucas Heights, Australia

^c Department of Nuclear Physics, Australian National University, Canberra, ACT 0200, Australia

^d Atominstytut, Vienna University of Technology, Austria

^e Institut für Kern- und Teilchenphysik, TU Dresden and FZ Rossendorf, Germany

^f European Commission, Joint Research Centre, Institute for Reference Materials and Measurements, B-2440 Geel, Belgium

^g Paul Scherrer Institute, 5232 Villigen PSI, Switzerland

^h NAPC Nuclear Data Section, International Atomic Energy Agency, A-1400 Vienna, Austria

ARTICLE INFO

Article history:

Received 12 August 2011

Received in revised form 18 March 2012

19 March 2012

Available online xxxxx

Keywords:

AMS

Reference material

Isobar-free AMS measurements

ABSTRACT

Isobaric interference represents one of the major limitations in mass spectrometry. For a few cases in AMS with tandem accelerators, isobaric interference is completely excluded like the well-known major isotopes ^{14}C , ^{26}Al , ^{129}I . Additional isotopes are ^{55}Fe ($t_{1/2} = 2.74$ years), ^{68}Ge ($t_{1/2} = 270.9$ days) and ^{202}Pb ($t_{1/2} = 52.5$ kyr), with ^{68}Ge and ^{202}Pb never been used in AMS so far. Their respective stable isobars, ^{55}Mn , ^{68}Zn and ^{202}Hg do not form stable negative ions. The exceptional sensitivity of AMS for ^{55}Fe , ^{68}Ge and ^{202}gPb offers important insights into such different fields like nuclear astrophysics, fundamental nuclear physics and technological applications. VERA, a dedicated AMS facility is well suited for developing procedures for new and non-standard isotopes. AMS measurements at the VERA facility established low backgrounds for these radionuclides in natural samples. Limits for isotope ratios of $<10^{-15}$, $<10^{-16}$ and $\leq 2 \times 10^{-14}$ were measured for $^{55}\text{Fe}/^{56}\text{Fe}$, $^{68}\text{Ge}/^{70}\text{Ge}$ and $^{202}\text{Pb}/\text{Pb}$, respectively. In order to generate accurate isotope ratios of sample materials, AMS relies on the parallel measurement of reference materials with well-known ratios. A new and highly accurate reference material for ^{55}Fe measurements with an uncertainty of $\pm 1.6\%$ was produced from a certified reference solution. In case of ^{68}Ge dedicated neutron activations produced a sufficiently large number of ^{68}Ge atoms that allowed quantifying them through the activity of its decay product ^{68}Ga . Finally, for ^{202}Pb , the short-lived isobar ^{202}Tl was produced via neutron activation and served as a proxy for ^{202}Pb AMS measurements.

© 2012 Elsevier B.V. All rights reserved.

1. Introduction

Isobaric interference represents one of the major limitations in mass spectrometry. In a few cases isobar-free AMS measurements with tandem accelerators are possible, and consequently lowest background levels are accessible. Such conditions are achieved if the isobar does not form stable negative ions either as an atomic ion or as a suitably-chosen molecular species; well-known examples are e.g. analyzing $^{14}\text{C}^-$, $^{26}\text{Al}^-$, $^{129}\text{I}^-$, or $^{41}\text{CaH}_3^-$, respectively, and similarly the radioisotopes in the mass range above Pb.

The above mentioned nuclides are commonly used in AMS in various applications since many years. We focus on some additional radionuclides with the same feature, namely allowing iso-

bar-free AMS measurements: ^{55}Fe ($t_{1/2} = 2.74$ years) [1], ^{68}Ge ($t_{1/2} = 270.9$ days) [2] and ^{202}Pb ($t_{1/2} = 52.5$ kyr) [3]. It was demonstrated by Korschinek et al. [4] that ^{55}Mn does not form stable negative ions, and recently first AMS measurements at the VERA facility, Univ. of Vienna, were performed with applications in nuclear astrophysics and nuclear technology [5,6].

No AMS measurements are reported so far for ^{68}Ge and ^{202}Pb . However, it is well-known that the electron affinities of Zn and Hg are <0 [7], thus the stable isobars of ^{68}Ge and ^{202}Pb , ^{68}Zn and ^{202}Hg , respectively, should not form stable negative ions, too. We report here on first AMS measurements at VERA of ^{68}Ge and ^{202}Pb and demonstrate their applicability with some first applications (Sections 3 and 4).

VERA, a dedicated AMS facility, based on a 3-MV tandem and featuring high mass resolution in combination with efficient background suppression and an automated measurement procedure, allows to transport all nuclides from hydrogen to the actinides to

* Corresponding author at: VERA Laboratory, Faculty of Physics, University of Vienna, Währinger Strasse 17, A-1090, Austria.

E-mail address: anton.wallner@anu.edu.au (A. Wallner).

the detector stations. Such a facility is well suited for developing the tuning and measurement procedures for new and non-standard isotopes. It is also designed to generate highly precise data. Since reference materials with well-known isotope ratios are required for optimum applications of these new and exotic radionuclides, we have produced dedicated AMS reference materials for all three isotopes.

2. Production of a new ^{55}Fe ($t_{1/2} = 2.74$ years) reference material

^{55}Fe ($t_{1/2} = 2.744 \pm 0.009$ years) [1] is not a new radionuclide to AMS. Korschinek et al. have shown that its stable isobar ^{55}Mn does not form stable negative ions [4]. Although rather short-lived for an AMS nuclide, its decay pattern (pure electron capture without γ -emission) makes decay counting feasible only via chemical separation and X-ray counting using a Si(Li) detector [8] or liquid scintillation counting (LSC) [9]. The extremely low background in ^{55}Fe measurements observed with AMS, however, allows sensitive ^{55}Fe detection [10]. We have demonstrated that ^{55}Fe measurements were reproducible to better than 1%. If selecting Fe^- , ^{55}Mn is completely suppressed. While FeO^- provides somewhat higher currents (up to several μA), Fe^- still allows to extract currents between several hundreds of nA and up to $1.5 \mu\text{A}$ $^{56}\text{Fe}^-$. We usually selected the 3^+ charge state because of the higher yield of $\approx 20\%$ at 3.0 MV terminal voltage compared to the 4^+ or 5^+ with 12% and 6% yield, respectively [10].

Our previous ^{55}Fe measurements, though highly precise, still suffered from the lack of a well-known reference material. We normalized our data of unknown samples to ratios calculated from neutron activated Fe material. Although the calculation of the isotope ratio is straightforward, unfortunately, these reference materials were known to $\approx 8\%$ only, because the uncertainty of the thermal cross-section value itself is 8%.

Therefore, we decided to produce a new reference material with higher accuracy. A ^{55}Fe activity standard from PTB Braunschweig, Germany (No. 2000-1215) [11], certified to a specific activity of 287 kBq/g ($\pm 1.57\%$, 1σ) for a reference date of 1st Oct. 2008 was used as starting material. The standard was in the form of $^{55}\text{FeCl}_3$ dissolved in 2.0022 g of aqueous solution. Taking a half-life of (1002 ± 3) days [11] we calculate a total number of $(7.18 \pm 0.12) \times 10^{13}$ ^{55}Fe atoms. Four Fe foils of natural isotopic composition (Goodfellow Ltd., item No. FE000406, high purity 99.9 + %, $5 \text{ cm} \times 5 \text{ cm} \times 0.5 \text{ mm}$) with masses accurately measured (see Table 1) were dissolved in HCl and FeCl_3 was formed. The solution with the ^{55}Fe activity standard was added to one of these FeCl_3 solutions (foil Fe-3, $M_{\text{Fe}} = 9.8616$ g). To ensure complete transfer the ampoule containing the ^{55}Fe solution was washed several times with bi-distilled water which was also added to the FeCl_3 solution. A total mass of 9.8616 g Fe corresponds to 9.758×10^{22} ^{56}Fe atoms (natural abundance of $^{56}\text{Fe} = 91.754\%$ and a molar mass of $^{56}\text{Fe} = 55.845$, [12]). From these two numbers we calculate an

isotope ratio $^{55}\text{Fe}/^{56}\text{Fe}$ $(7.36 \pm 0.12) \times 10^{-10}$. This solution represents our master solution A0. By taking aliquots (see Table 1) from this master solution and adding them to two remaining FeCl_3 solutions which contain the other dissolved Fe foils (foils Fe-4, and Fe-2, respectively) we produced two additional reference materials A2 and A1 with isotope ratios $^{55}\text{Fe}/^{56}\text{Fe}$ of 2.34×10^{-10} and 5.77×10^{-12} , respectively (see Table. 1). Because the uncertainty of weighing the involved masses was negligible, all ^{55}Fe reference materials, A0, A1 and A2 are known to $\pm 1.6\%$, which is essentially the uncertainty of the ^{55}Fe activity standard (see Table. 1).

Important, ^{55}Fe is one of the radionuclides in AMS where a reference date for the activity and its isotope ratio is required, as decay corrections become significant on a month scale due to the short half-life of ca. 33 months. All isotope ratios are valid for a reference date of 1st Oct. 2008. The FeCl_3 solutions containing the three ^{55}Fe reference materials and the remaining blank solution (no ^{55}Fe was added to foil Fe-1) were then converted into solid form: under pH control FeOH was precipitated, dried and finally the material was ignited to produce Fe_2O_3 powder. Between 5 and 10 g of powder was produced for each of the three reference materials and the ^{55}Fe blank. The two derivatives of the master solution A0, A2 and A1, were measured in a series of beam times with AMS at VERA and their measured results were compared to those measured for the master solution A0. They agreed within 1% (A2) and 2.5% (A1) with the calculated values and thus confirmed the quoted isotope ratios table 1.

A different approach for producing a $^{55}\text{Fe}/^{54}\text{Fe}$ reference material was applied as well: highly enriched ^{54}Fe metal foils and ^{54}Fe powder samples were exposed to a proton beam of 4 and 5.5 MeV particle energy, respectively. Via a (p,γ) reaction radioactive ^{55}Co was produced. ^{55}Co decays to 100% to ^{55}Fe with a half-life of 17.54 h. After the proton irradiation, the activity of ^{55}Co in the ^{54}Fe samples was measured with a HP Ge diode with well-known γ -ray efficiency ($\pm 2.5\%$). From that quantity the number of ^{55}Co atoms in the sample was calculated, which – after an appropriate waiting time – corresponds to the total number of the decay products ^{55}Fe . Including all uncertainties, the final $^{55}\text{Fe}/^{54}\text{Fe}$ isotope ratios for these reference samples were known to $\pm 5\%$. These “ ^{54}Fe -samples” and a batch of available ^{55}Fe powder material produced previously from neutron activations (see above) were cross-calibrated to the above mentioned master solution A0. To summarize, a large amount of well-known ^{55}Fe reference materials with $^{55}\text{Fe}/\text{Fe}$ isotope ratios between 6×10^{-13} and 7×10^{-10} was produced and is available for AMS measurements.

Recently, we have applied AMS for studying the production of ^{55}Fe in stellar nucleosynthesis [5,13,14]. Additional applications comprise detailed studies of ^{55}Fe production in a fusion environment: via fast neutron induced reactions on ^{58}Ni and ^{56}Fe , ^{55}Fe is produced through (n,α) and $(n,2n)$ reactions, respectively [6,15]. We measured cross sections for ^{55}Fe production under such conditions: natural Fe samples were irradiated at TU Dresden [16] with neutrons between 13.4 and 14.8 MeV, and at IRMM [17] from 13 to

Table 1
Isotope ratios for our new ^{55}Fe reference materials: the activity standard from PTB itself contained 58 mg/L FeCl_3 , which is negligible (0.04 mg) compared to the ≈ 10 g added. Note, A2 and A1 contain fractions of A0 ($f(\text{A0})$, 47.4% and 0.79%, respectively), therefore the total number of ^{56}Fe atoms is higher than calculated from the mass of the Fe foil only. The final uncertainty of the ^{55}Fe reference material was calculated to $\pm 1.6\%$. Subsequent AMS measurements confirmed the calculated ratios of A2 and A1 relative to A0. The number of ^{55}Fe atoms was calculated from the certified activity of 287 kBq/g using a half-life value of (1002 ± 3) days.

Sample	$M_{\text{Fe foil}} [\text{g}]$	$N_{^{56}\text{Fe}} (\text{atoms})$	$N_{^{55}\text{Fe}} (\text{atoms})^*$	$^{55}\text{Fe}/^{56}\text{Fe}^*$	Remarks
PTB- ^{55}Fe		3.965×10^{17}	$7.18 \pm 0.12 \times 10^{13}$		Activity std.
A0	9.8616	9.758×10^{22}	7.179×10^{13}	$(7.36 \pm 0.12) \times 10^{-10}$	PTB + Fe-3
A2	10.0066	1.453×10^{23}	3.405×10^{13}	$(2.34 \pm 0.04) \times 10^{-10}$	$f(\text{A0}) + \text{Fe-4}$
A1	9.8512	9.824×10^{22}	5.673×10^{11}	$(5.77 \pm 0.09) \times 10^{-12}$	$f(\text{A0}) + \text{Fe-2}$
Blank	9.8922	9.788×10^{22}	–	$< 10^{-15}$	Fe-1

* Note: all numbers are valid for a reference date 1st Oct. 2008.

20 MeV. Final results for $^{56}\text{Fe}(n,2n)^{55}\text{Fe}$ and $^{58}\text{Ni}(n,\alpha)$ cross sections are precise at a level of <4% [14].

3. ^{68}Ge ($t_{1/2} = 271$ days)

3.1. General aspects of AMS measurements of ^{68}Ge

^{68}Ge is the longest-lived radioisotope of Ge with a half-life of (270.95 ± 0.16) days [2] (not counting the double-beta decay nuclide ^{76}Ge with a half-life of 1.5×10^{21} years, Fig. 1). Similar to ^{55}Fe , ^{68}Ge decays via pure electron capture (EC), directly to the ground state of ^{68}Ga without emission of any γ -radiation. ^{68}Ga itself is radioactive and decays with a half-life of 68 min via β^+ and EC primarily to the ground state of stable ^{68}Zn . Only a small fraction (3%) decays to an excited state at 1077 keV and is therefore associated with a characteristic γ -emission line (some higher excited states are populated as well with a probability <0.4%). ^{68}Ge is the parent in the $^{68}\text{Ge}/^{68}\text{Ga}$ generator (see e.g. [18,19]), well-known for positron emission therapy (PET). As such large amounts of ^{68}Ge are produced world-wide. Various production methods via charged particle induced reactions are applied to generate ^{68}Ge artificially: e.g. $^{nat}\text{Ga}(p,2n)^{68}\text{Ge}$ or α -induced reactions on Zn (e.g. $^{66}\text{Zn}(\alpha,2n)^{68}\text{Ge}$). In nature, ^{68}Ge is produced at very low amounts by cosmic-ray produced neutrons impinging with high energies on ^{nat}Ge and forming ^{68}Ge via (n,xn) reactions ($^{nat}\text{Ge}(n,xn)^{68}\text{Ge}$).

The stable isobar to ^{68}Ge is ^{68}Zn . As for ^{55}Fe , also ^{68}Ge does not either suffer from isobaric interference in AMS measurements because Zn does not form stable negative ions. First tests at VERA verified that Zn^- is indeed not detected in the beam. ^{68}Ge ($Z = 32$, $N = 36$) is two mass units below the first stable Ge isotope ^{70}Ge (20.38% abundance). Therefore, any Ge isotope can only form molecules higher in mass and the beam of mass $A = 68$ injected into the tandem accelerator will essentially be free of other Ge isotopes (a very small fraction of scattered ions might exist, however). The stable isobar of ^{68}Ge , ^{68}Zn is two atomic units lower ($Z = 30$).

Elemental Ge forms a very prolific negative ion [20] and produces excellent currents. The atomic electron affinity for Ge is high (1.23 eV, compared to Fe with 0.15 eV) [7]. We could easily extract several μA of $^{70}\text{Ge}^-$, i.e. 5–15 μA of total Ge currents. We did not observe any difference in sputtering behavior and overall performance using either large pieces of Ge crystal crushed into small grains or fine Ge powder. Usually, Ge was pressed without any binder into the sample holder. In contrast to ^{55}Fe measurements, Ge currents measured with Faraday cups are all from higher masses compared to ^{68}Ge . Note, the decay product ^{68}Ge will quickly be in radioactive equilibrium with ^{68}Ge , with a $^{68}\text{Ga}/^{68}\text{Ge}$ ratio of 1.8×10^{-4} . However, Ga does not form negative ions as readily as Ge, thus detector counts will be almost exclusively from ^{68}Ge and not from its decay product ^{68}Ga .

Tuning was performed with stable ^{70}Ge . For the final setup attenuated beams of both $^{70}\text{Ge}^{5+}$ and $^{72}\text{Ge}^{5+}$ were directed into the particle detector (ionization chamber) for optimizing the measurement setup and for scaling the energy signals from those runs to the energy region of interest expected for the rare ^{68}Ge events. Usually, we selected also ^{70}Ge , the isotope with the closest mass, for the current measurements. In fast switching mode ^{70}Ge was bounced into the low energy and high-energy offset Faraday cups at VERA. Either the 3^+ or the 5^+ charge state was selected for the measurements; while 4^+ for $A = 68$, i.e. $68/4 = 17$, results in background originating from lower charge states. We usually utilized our compact $\Delta E/E$ ionization chamber [21] for Ge measurements. As expected, detector count rates were very low for blank samples (see below). At VERA we selected a terminal voltage of 2.9 MV. The 3^+ ions had 11.66 MeV and correspondingly 5^+ ions 17.46 MeV par-

ticle energy. It turned out that both charge states were comparable in their performance.

3.2. Natural Ge blank material

We investigated different Ge materials: commercially available Ge powder and Ge grains (Alfa Aesar, Goodfellow); also a larger piece from a Ge crystal was available. They were pressed into both Al and Cu sample holders. No additional powder was added to the Ge sputter samples and all different kinds of investigated samples performed well.

AMS results obtained at VERA for such blank samples are plotted in Fig. 2. Most of the runs were essentially without any detector events. Rarely an event was registered, which could be either a real ^{68}Ge ion or also an ion which mimics a true event. Such events seemed to be more frequent for runs performed directly after sputtering reference samples for a longer time. Also, Cu and Al blank samples (both empty sample holders and Cu and Al_2O_3 powder pressed into sample holders) gave the same (low) number of detector events as the ^{nat}Ge (blank) samples. Thus, most likely, these rare events are originating from contamination in the ion source indicating a cross talk or memory effect of the order of 10^{-4} or less.

As indicated in Fig. 2, most of the runs on such Ge blank samples did not result in any ^{68}Ge event. A typical Ge sputter sample (~ 10 mg) lasted about 2 h. The mean values for such blank samples in four different measurement series was $^{68}\text{Ge}/^{70}\text{Ge} < 7 \times 10^{-16}$ (measurement series I, 6 blank sputter cathodes, no detector event), $(3 \pm 2) \times 10^{-16}$ (measurement series II, 14 blank cathodes, 3 detector events), $(5 \pm 3) \times 10^{-16}$ (measurement series III, 8 blank cathodes, 5 detector events) and $(0.4 \pm 0.6) \times 10^{-16}$ (measurement series IV, 10 sputter cathodes, 1 detector event), respectively. Upper limits and isotope ratios for such low-event-number measurements were calculated applying the statistics of Feldman & Cousin [22]. In total nine events were registered for those blank samples and interestingly, all these events originate from sputter samples which were pressed into Al sample holders (note: Ga is the chemical homolog of Al, thus some Ga might be present in the sample holder. It cannot be excluded that naturally produced ^{68}Ga (e.g. via $(n,2n)$ on stable ^{69}Ga) will result in some very rare detector events).

No detector event was registered from any material pressed into Cu samples holder. However, due to the low number of counts, this might just be coincidence. In addition, 3 out of the 5 events registered in measurement series III were obtained after a long sputtering time on reference samples with isotope ratios $^{68}\text{Ge}/^{70}\text{Ge}$ of a few 10^{-12} . Although on the limit of significance, this “higher frequency” may originate from cross contamination in the ion source and this finding fits to the conclusion for ^{68}Ge events registered for pure (empty) Al and Cu sample holders (see above). In the first measurement series, no reference sample was measured together with the unknown samples, and in the last measurement series (IV), after a short beam tuning, only one reference sample ($^{68}\text{Ge}/^{70}\text{Ge} \sim 10^{-12}$) was measured together with a large number of samples low in ^{68}Ge content.

Such low background levels in combination with Ge currents of a few μA makes AMS a sensitive tool for ^{68}Ge measurements and it is basically limited by the number of ^{68}Ge atoms in the sputter sample. If we assume an overall AMS efficiency of 5% (conservative estimate, the electron affinity of Ge is almost identical to that of carbon) and 10^4 ^{68}Ge atoms available in a 1 mg ^{nat}Ge sample, we expect 50 detector counts from that sample if fully consumed; these numbers corresponds to an isotope ratio of $^{68}\text{Ge}/^{70}\text{Ge} = 6 \times 10^{-15}$, well above the ratios found for blank samples. Moreover, that sample is measured in less than 1 h. For comparison, 10^4 ^{68}Ge atoms correspond to an activity of 0.3 mBq (or one 1077 keV γ -ray emitted per day). Only pure Ge metal samples

As 67 42.5 s β^+ 4.7; 5.0... γ 123; 121; 244...	As 68 2.53 m β^+ 4.7; 6.1... γ 1016; 762; 651; 1778...	As 69 15.1 m β^+ 3.0... γ 233; 146; 87...	As 70 53 m β^+ 2.1; 2.8... γ 1040; 668; 1114; 745; 1708; 2020...	As 71 65.28 h ϵ β^+ 0.8... γ 175; 1095...	As 72 26.0 h β^+ 2.5; 3.3... γ 834; 630...	As 73 80.3 d ϵ no β^+ γ 53...	As 74 17.77 d ϵ β^+ 0.9; 1.5... β^- 1.4... γ 596; 635...	As 75 100 σ 4.0
Ge 66 2.3 h ϵ β^+ 0.7; 1.1... γ 382; 44; 109; 273...	Ge 67 18.7 m β^+ 3.0; 3.2... γ 167; 1473...	Ge 68 270.82 d ϵ no β^+ no γ σ 1.0	Ge 69 39.0 h ϵ β^+ 1.2... γ 1107; 574; 872; 1336...	Ge 70 20.38 σ 3.0	Ge 71 11.43 d ϵ no γ	Ge 72 27.31 σ 0.9	Ge 73 7.76 σ 15	Ge 74 36.72 σ 0.14 + 0.28
Ga 65 15 m β^+ 2.1; 2.2... γ 115; 61; 153; 752...	Ga 66 9.4 h β^+ 4.2... γ 1039; 2752; 834; 2190; 4296...	Ga 67 78.3 h ϵ no β^+ γ 93; 185; 300...	Ga 68 67.63 m β^+ 1.9... γ 1077; (1833)	Ga 69 60.108 σ 1.68	Ga 70 21.15 m β^- 1.7... ϵ γ (1040; 176)	Ga 71 39.892 σ 4.7	Ga 72 14.1 h β^- 1.0; 3.2... γ 834; 2202; 630; 2508...	Ga 73 4.86 h β^- 1.2; 1.5... γ 287; 53; 326... ϵ
Zn 64 48.268 σ 0.74 $\sigma_{n,p}$ α 1.1E-5 $\sigma_{n,p}$ α <1.2E-5	Zn 65 244.3 d ϵ ; β^+ 0.3 γ 1115... σ 66 $\sigma_{n,p}$ α 2.0	Zn 66 27.975 σ 0.9 $\sigma_{n,p}$ α <2E-5	Zn 67 4.102 σ 6.9 $\sigma_{n,p}$ α 0.0004	Zn 68 19.024 σ 0.072 + 0.8 $\sigma_{n,p}$ α <2E-5	Zn 69 13.8 h 56 m β^- 4.39 β^- 0.9 γ (574); (319)	Zn 70 0.631 σ 0.0081 + 0.083	Zn 71 2.4 m β^- 1.5; 2.5... γ 386; 487; 620...	Zn 72 46.5 h β^- 2.8... γ 512; 910; 390...
Cu 63 69.15 σ 4.5	Cu 64 12.700 h ϵ ; β^- 0.6 β^+ 0.7 γ (1346) σ ~270	Cu 65 30.85 σ 2.17	Cu 66 5.1 m β^- 2.6... γ 1039; (834...) σ 140	Cu 67 61.9 h β^- 0.4; 0.6... γ 185; 93; 91...	Cu 68 3.8 m 30 s β^- 3.5; β^- 3.7; 4.6; 1.3 γ 1077; 1077...	Cu 69 3.0 m β^- 2.5... γ 1007; 834; 531...	Cu 70 6.6 s 33 s 44.5 s β^- 1.0; 3.5... γ 885; 101; 902; 141	Cu 71 19.5 s β^- 2.8... γ 490; 595; 587... σ g; m

Fig. 1. Chart of the nuclides [12] showing the mass region of interest for ^{68}Ge -AMS measurements. ^{68}Ge is the parent of the PET nuclide ^{68}Ga . The isobar ^{68}Zn does not form stable negative ions.

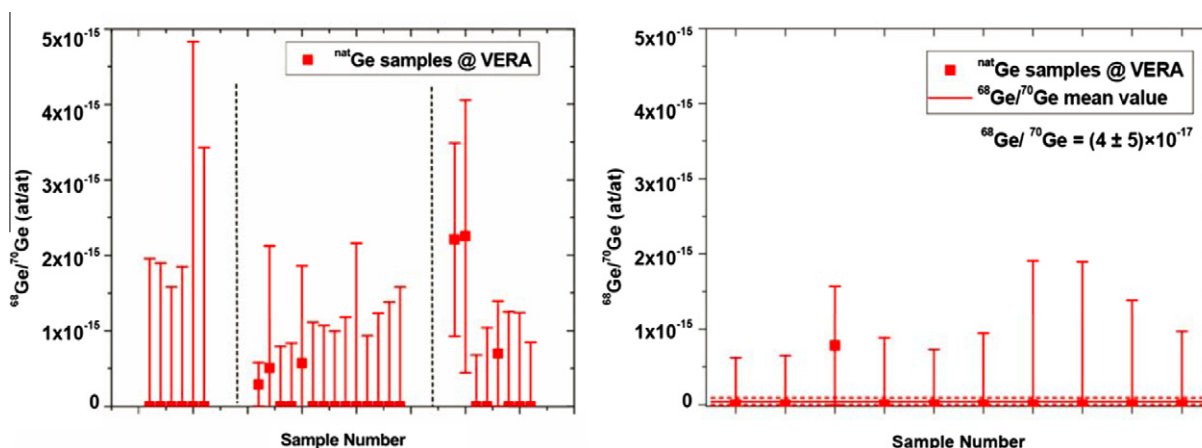


Fig. 2. Isotope ratios measured at VERA for $^{\text{nat}}\text{Ge}$ samples (blank samples). The left plot shows results from the first three measurement series, the plot on the right side results from a fourth measurement. The mean $^{68}\text{Ge}/^{70}\text{Ge}$ isotope ratios in these four beam times were all low and between 0 and 5×10^{-16} .

were investigated so far. If sample preparation is required prior to AMS measurements some additional background ions cannot be excluded.

3.3. Reference material for ^{68}Ge measurements

The standard technique for quantifying larger amounts of ^{68}Ge is liquid scintillation counting. Other decay counting techniques like γ -counting suffer from the low γ -ray probabilities in this decay chain. For example 50 mg of $^{\text{nat}}\text{Ge}$ with an isotope ratio $^{68}\text{Ge}/^{70}\text{Ge}$ of 1×10^{-12} contain 8.4×10^{19} ^{70}Ge atoms, and 8.4×10^7 ^{68}Ge atoms. The latter number corresponds to an activity of 2.5 Bq. While LSC can easily handle such activities, γ -ray detection approaches its limits due to γ -rays only emitted in the decay of the daughter ^{68}Ga and here only with a probability of $\approx 3\%$. Dealing with significantly lower isotope ratios also makes LSC challenging.

We produced a reference material for ^{68}Ge measurements by bombarding $^{\text{nat}}\text{Ge}$ material with highly energetic neutrons at PSI (590 MeV protons were impinging on a massive Pb spallation target and produced a white neutron spectrum from thermal up to 590 MeV [23]). ^{68}Ge was produced via (n,xn) reactions on the stable Ge isotopes. The first stable isotope in mass to ^{68}Ge is ^{70}Ge , and

followed by $^{72,73,74,76}\text{Ge}$ (see Fig. 1). The neutron threshold energy for $^{70}\text{Ge}(n,3n)$ is 20.01 MeV. For the other isotopes much higher neutron energies for ^{68}Ge production are required, between 38.42 and 71.74 MeV. For the production of reference materials, samples with masses of ≈ 100 mg Ge with natural isotopic composition were exposed to these spallation neutrons with irradiation times between 1 min and 1 h. The samples with the highest isotope ratios ($>10^{-12}$) were accessible to decay counting. Their number of produced ^{68}Ge was measured through the γ -rays emitted in the decay of the daughter nuclide ^{68}Ga . $^{68}\text{Ge}/^{70}\text{Ge}$ isotope ratios between 10^{-14} and 10^{-12} were obtained in these neutron irradiations; with the lower isotope ratios cross-calibrated via AMS relative to the “ 10^{-12} samples”.

3.4. First application: Measurement of the $^{70}\text{Ge}(n,3n)^{68}\text{Ge}$ cross section near threshold

^{68}Ge is in nature – at very low levels – produced predominantly via (n,xn) reactions on $^{\text{nat}}\text{Ge}$ with highly energetic neutrons, as secondary products from primary cosmic rays. For studying the most likely production channel in nature, the $^{70}\text{Ge}(n,3n)^{68}\text{Ge}$ reaction, which has its threshold at a neutron energy of 20.01 MeV, $^{\text{nat}}\text{Ge}$

samples were irradiated with quasi-mono-energetic neutrons at IRMM, Belgium [17]. The irradiations were carried out with the 7 MV Van de Graaff accelerator. Neutrons with energies of 18.8, 21 and 22 MeV were produced via the ${}^3\text{H}(\text{d},\text{n}){}^4\text{He}$ reaction ($Q = 17.59$ MeV) using a solid-state Ti/T target of 2 mg/cm^2 thickness on a gold backing of 0.5 mm thickness. In total, three different Ge samples were irradiated with neutron energies around the threshold of the $(\text{n},3\text{n})$ reaction.

First results from AMS measurements showed no ${}^{68}\text{Ge}$ detector events for samples irradiated with neutrons below the $(\text{n},3\text{n})$ threshold. The sample irradiated with 22 MeV, however, indicates isotope ratios ${}^{68}\text{Ge}/{}^{70}\text{Ge}$ of a few times 10^{-15} , clearly above background. These measurements are in progress now.

Recently, we have investigated the Ge performance with a different AMS setup, with the ANTARES accelerator [24] at ANSTO. The same Ge material as analyzed at VERA was sputtered, and again Ge^- was injected into the FN tandem, which was operated at 3.62 MV. The 3^+ charge state was selected which gave a high charge state yield of 22–23% (at VERA most measurements were performed with the 5^+ charge state). Two different blank samples (Ge powder and Ge grains, both from Alfa Aesar) gave no counts in runs of more than 1 h. Both measurements gave upper limits of ${}^{68}\text{Ge}/{}^{70}\text{Ge} < 5 \times 10^{-16}$ (according to Feldman and Cousins, [22]). The reference material gave the same results as measured at VERA. Interestingly, sample holders made of pure Al, which served as pure blank samples in these measurements, showed measurable Ge currents of some nA. Currents for different masses reproduced the isotopic abundance ratios of the stable Ge isotopes. Compared to the μA of Ge current obtained from the Ge samples, such currents as extracted from the Al sample holder, however, represent of the order of ‰ contamination with Ge.

4. ${}^{202}\text{gPb}$ ($t_{1/2} = 52,500$ years)

4.1. General aspects of AMS measurements of ${}^{202}\text{gPb}$

${}^{202}\text{gPb}$ is a long-lived isotope which is rather rarely used in science and technology. Since a few years, it has been applied for precise isotopic analysis of Pb in sub-nanogram quantities by thermal ionization mass spectrometry (TIMS). Here, a ${}^{202}\text{Pb}$ - ${}^{205}\text{Pb}$ -double spike is used for TIMS analysis of Pb which allows an internal fractionation correction for U-Pb dating of various rocks, minerals, and meteorites [25]. In addition, a short-lived isomer, ${}^{202\text{m}}\text{Pb}$ exists, which, however, decays with a half-life of 3.62 h directly (100%) to unstable ${}^{202}\text{Tl}$ ($t_{1/2} = 12.23$ days) (see Fig. 3).

Previous Pb measurements with AMS were performed mainly for ${}^{205}\text{Pb}$ ($t_{1/2} = 15$ Myr) [26] at GSI-UNILAC in a geochemical experiment where ${}^{205}\text{Tl}$ was suggested as a solar neutrino detector. For such measurements, the major difficulty was the separation of the stable isobar ${}^{205}\text{Tl}$. AMS measurements of ${}^{205}\text{Pb}$ requires the highest particle energies available; thus AMS at GSI was the only approach so far. The passive absorber technique was used and particles with energies of 11.4 MeV/u (2.34 GeV) were analyzed achieving a suppression factor of about 1000 for ${}^{205}\text{Tl}$.

In contrast to ${}^{205}\text{Pb}$, ${}^{202}\text{gPb}$ measurements do not suffer from isobaric interference, if Pb^- is selected. The stable isobar, ${}^{202}\text{Hg}$, does not form stable negative ions and thus no interference from ${}^{202}\text{Hg}$ is expected. Therefore, much lower particle energies are sufficient compared to ${}^{205}\text{Pb}$ measurements and standard AMS facilities can be utilized. ${}^{202}\text{Pb}$, similarly to ${}^{68}\text{Ge}$, is two mass units lower than the lightest stable Pb isotope, ${}^{204}\text{Pb}$, which has a natural abundance of 1.4% only. Tl ($Z = 81$), is one charge unit lower than Pb, and has two stable isotopes with $A = 203$ and 205, which are also higher in mass than the radionuclide ${}^{202}\text{Pb}$ (see Fig. 3). Therefore, con-

sidering close-by isotopes, only Hg can form molecules (e.g. hydrides) which may be injected into the tandem if mass 202 is analyzed. To summarize, ${}^{202}\text{Pb}$ measurements are expected to be isobar-free, and there is a low chance for neighboring isotopes to be injected into the tandem accelerator and eventually be transported to the particle detector. Hence, we expect a very low background for ${}^{202}\text{Pb}^-$ AMS measurements. This case is different to other heavy isotope measurements being also in fact isobar-free, but where interference from neighboring masses limits the sensitivity of AMS. For example, ${}^{236}\text{U}$ measurements are often limited by interference from ${}^{235}\text{UH}$ molecules, and a low energy tail of leaky ${}^{235}\text{U}$ in the time-of-flight spectrum [27–31]. This effect is even more pronounced in case of AMS measurements of ${}^{210\text{m}}\text{Bi}$ where the isotope ${}^{209}\text{Bi}$ is interfering also one mass unit lower, and in contrast to ${}^{235}\text{U}$ (0.72%), ${}^{209}\text{Bi}$ is the only stable isotope.

Lead has a small electron affinity (E.A. = 0.364 eV) [7] and sputters very quickly [20]. Although elemental Pb performs poorly compared to molecules, we were able to extract ${}^{208}\text{Pb}^-$ currents up to 30 nA (similar values were observed for highly enriched ${}^{204}\text{Pb}^-$, see Section 4.4). The 4^+ charge state was selected, which was formed with a charge state yield of about 5–6% and correspondingly, currents between 1 and 4 nA ${}^{208}\text{Pb}^{4+}$ were measured at the high energy side. At VERA lead measurements were performed in the same way as e.g. ${}^{236}\text{U}$ measurements, utilizing the heavy-ion beamline featuring a 2.8-m flight path for TOF measurement and a Bragg-type ionization chamber for the energy measurement [32].

4.2. Pb blank material

We investigated commercially available natural lead material, both metallic foils and Pb powder as blank materials for ${}^{202}\text{gPb}$ measurements. Lead is soft and metallic foils can easily be pressed into sample holders. Results from two AMS beam times at VERA for such Pb blank measurements are plotted in Fig. 4: 11 and 15 sputter samples were measured, all between 1 and 2 h of sputtering time each. Only one count was registered in the first measurement series, none in the second. The measured isotope ratios for these blank samples were ${}^{202}\text{Pb}/\text{Pb} = 2 \times 10^{-14}$ and $< 10^{-13}$, respectively. For natural lead, ${}^{208}\text{Pb}^-$ was analyzed as the stable reference isotope. These low background values confirm the expected performance of Pb^- measurements at VERA.

4.3. Reference material for ${}^{202}\text{Pb}$ measurements

A reference material for ${}^{202}\text{gPb}$ AMS measurements was not available for these measurements. Therefore, we used the short-lived isobar ${}^{202}\text{Tl}$ ($t_{1/2} = 12.2$ days) as a proxy for the beam transmission of ${}^{202}\text{Pb}$ at the high energy side. To this end, highly enriched ${}^{203}\text{Tl}$ was irradiated with neutrons and via $(\text{n},2\text{n})$ ${}^{202}\text{Tl}$ was produced. Due to the high production cross section of ${}^{202}\text{Tl}$ for 14–20 MeV neutrons and its short half-life, a measurable activity of ${}^{202}\text{Tl}$ was obtained. Detection of the dominant γ -line at 439.6 keV (94%) associated with the decay of ${}^{202}\text{Tl}$ allowed calculation of the amount of ${}^{202}\text{Tl}$ isotopes in that sample. In combination with the well-known mass of the Tl sample, ${}^{202}\text{Tl}/{}^{203}\text{Tl}$ isotope ratios were calculated with uncertainties between 5% and 7%. Neutron irradiations of ${}^{203}\text{Tl}$ were performed also at IRMM [17], in parallel with ${}^{204}\text{Pb}$ activations (see Section 4.4, below). In addition, a dedicated activation was performed at TU Dresden's 14-MeV neutron generator [16]. Therewith, ${}^{202}\text{Tl}/{}^{203}\text{Tl}$ isotope ratios of $(0.7\text{--}3) \times 10^{-11}$ were produced in these irradiations. For a 30 mg enriched ${}^{203}\text{Tl}$ sample and an isotope ratio of 1×10^{-11} , an activity of about 580 Bq was generated, easily measurable with a conventional HP Ge detector. However, because of the short half-life of ${}^{202}\text{Tl}$, its production, the activity measurement and subsequent

Po 203 45 s 36 m ε: β ⁺ α 5.394 γ 906; 1091; 894 hy 641... 215...	Po 204 3.53 h ε: β ⁺ α 5.377 γ 884; 270; 1016...	Po 205 1.66 h ε: β ⁺ α 5.22; α → g γ 872; 1001; 850; 837...	Po 206 8.8 d ε: β ⁺ α 5.2233 γ 1032; 511; 286; 807... e ⁻ : g	Po 207 2.8 s 5.84 h ε: β ⁺ α 5.116 γ 992; 743; 912...; g h 815; 288; 301	Po 208 2.898 a ε: β ⁺ α 5.1152... γ (292; 571...) g	Po 209 102 a ε: β ⁺ α 4.981... γ (895; 261; 263...)	Po 210 138.38 d ε: β ⁺ α 5.90439; 8853... γ (803); α <0.0005 γ <0.030; β _{max} α 0.002; α ₁ <0.1	Po 211 25.2 s 0.516 s ε: β ⁺ α 7.275; 8853... γ 7.450... 1094... γ (898; 570...)
Bi 202 1.72 h ε: β ⁺ γ 961; 422; 657... g	Bi 203 11.76 h ε: β ⁺ 1.4... γ 820; 825; 897; 1848... g; m	Bi 204 11.22 h ε: β ⁺ γ 899; 375; 984... g; m	Bi 205 15.31 d ε: β ⁺ γ 1764; 703; 988...	Bi 206 6.24 d ε: β ⁺ γ 803; 881; 516; 1719; 537...	Bi 207 31.55 a ε: β ⁺ γ 570; 1064; 1770...	Bi 208 3.68 · 10 ⁵ a ε: β ⁺ γ 2615	Bi 209 100 rr 0.011 + 0.023 β _{max} α <3E-7	Bi 210 3.0 · 10 ⁵ a 5.013 d ε: β ⁺ 1.2 α 4.946; α 4.540; γ 296; 304...; γ (305; 266...)
Pb 201 61 s 9.4 h ε: β ⁺ γ 331; 361; 546... hy 523	Pb 202 3.62 h 5.25 · 10 ⁴ a ε: β ⁺ γ 961; 422; 767...; ε γ 490; 460; 390 no γ	Pb 203 6.2 s 51.9 h ε: β ⁺ γ 825; 401... hy 825; 401... 375... rr 0.68	Pb 204 67.2 m 1.4 ε: β ⁺ hy 899; 912; 375... rr 0.68	Pb 205 1.5 · 10 ⁷ a ε: β ⁺ no γ; g rr ~5	Pb 206 24.1 ε: β ⁺ rr 0.027	Pb 207 22.1 ε: β ⁺ rr 0.61	Pb 208 52.4 rr 0.00023 β _{max} α <3E-6	Pb 209 3.253 h ε: β ⁺ 0.6 no γ
Tl 200 26.1 h ε: β ⁺ γ 368; 1206; 579; 828... g	Tl 201 73.1 h ε: β ⁺ γ 167; 135... g	Tl 202 12.23 d ε: β ⁺ γ 440; (520...) g	Tl 203 29.52 ε: β ⁺ rr 11 β _{max} α <0.0003	Tl 204 3.78 a ε: β ⁺ 0.8; ε no γ; g rr 22	Tl 205 70.48 ε: β ⁺ rr 0.11	Tl 206 3.7 m 4.20 m ε: β ⁺ hy 898; 453; 210; 256; 1021... β ⁺ 1.5... γ (803...)	Tl 207 1.33 s 4.77 m ε: β ⁺ hy 1000; 351 β ⁺ 1.4... γ (898...)	Tl 208 3.053 m ε: β ⁺ 1.8; 2.4... γ 2615; 583; 511; 860; 277...
Hg 199 42.5 m 15.87 h 158; 374... e ⁻ α 2100	Hg 200 23.10 rr ~1	Hg 201 13.18 rr ~8	Hg 202 29.86 rr 4.9	Hg 203 46.59 d ε: β ⁺ 0.2 γ 279	Hg 204 6.87 ε: β ⁺ rr 0.4	Hg 205 5.2 m ε: β ⁺ 1.5... γ 204...	Hg 206 8.15 m ε: β ⁺ 1.5... γ 305; 650... g	Hg 207 2.9 m ε: β ⁺ 1.8... γ 351; 997; 1637... m; g

Fig. 3. Chart of the nuclides showing the mass region of interest for ²⁰²Pb-AMS measurements. The isobar ²⁰²Hg does not form stable negative ions [12].

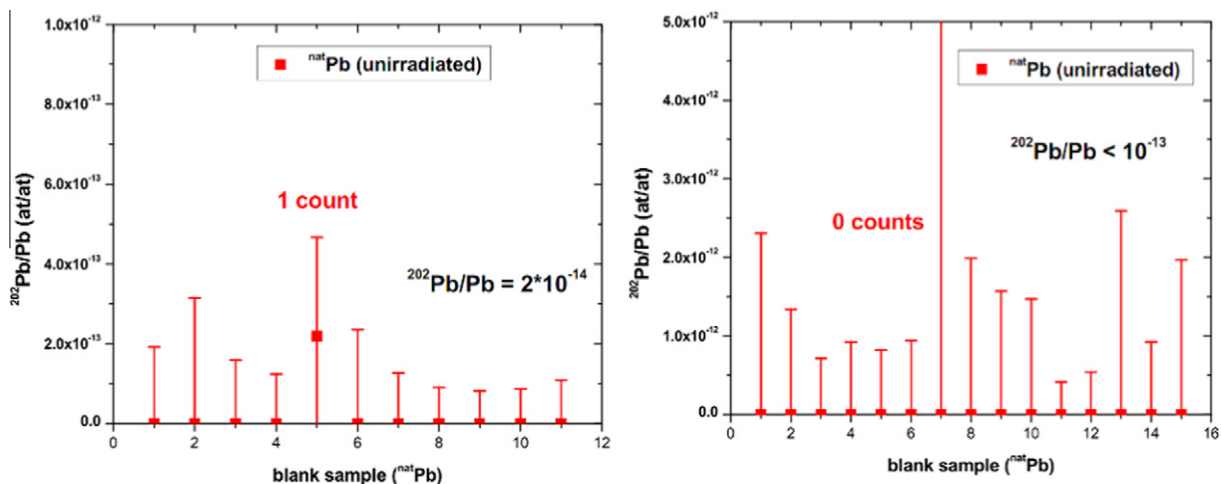


Fig. 4. Isotope ratios measured at VERA for ^{nat}Pb samples (blank samples). The left plot shows results from a first measurement series (11 blank samples), the plot on the right side results from a second measurement (15 blank samples). The ²⁰²Pb/Pb isotope ratios were all low with $(2 \pm 3) \times 10^{-14}$ and $< 10^{-13}$, respectively. Only one count was registered in total.

AMS usage had to be organized in a timely manner, and were performed directly after each other.

Tl does not form negative ions readily (its electron affinity is even lower than that of Pb, (0.2 eV, compared to 0.36 eV) [21]. In order to serve as proxy for ²⁰²Pb, ²⁰²Tl measurements required the usage of the elemental ion as well, to completely suppress ²⁰²Hg isobaric interference. Typical currents were between a few and up to 15 nA ²⁰³Tl⁻, corresponding to 1–3 nA ²⁰³Tl⁴⁺.

4.4. First application: measurement of the ²⁰⁴Pb(n,3n)²⁰²Pb cross section near threshold

Lead in general is of interest for both, developments in nuclear physics and for applications: (i) in nuclear physics the closed proton shell of lead had led to numerous studies of nuclear structure and nuclear reactions to test and develop nuclear models; (ii) in engineering and research lead is found everywhere for shielding against gamma-radiation, and also in neutron environments; (iii) in advanced reactors liquid lead is proposed as a possible coolant alternative to sodium or gas; and (iv) in accelerator driven systems lead is part of the proposed spallation target (e.g. as lead–bismuth–

eutectic or as liquid lead). Due to the high neutron flux in such systems in combination with the high proton and neutron energies (several 100 MeV, typically), nuclear reactions will produce all kind of nuclides close to the target elements. Consequently, a mixed waste is generated which complicates the spallation target disposal. In particular, via neutron capture ^{210m}Bi ($t_{1/2} = 3.0$ Myr) will be produced, and via spallation processes the long-lived radioisotopes ²⁰²Pb, ²⁰⁵Pb, and ¹⁹⁴Hg will be produced. Calculations show that after 10⁴-years cooling time, the dominant radionuclide, representing 50% of the activity, is ²⁰²Tl, which is populated by the beta decay of the long-lived ²⁰²Pb. [33].

²⁰²Pb is produced via (n,xn) reactions. A particular feature of the lead isotopes in general are the low (n,2n) and (n,3n) thresholds. For instance (n,3n) channels are open well below 20 MeV neutron energy. The reaction ²⁰⁴Pb(n,3n)²⁰²Pb is an example of a reaction that could not be studied before (no experimental data available) because the end product is long-lived (5.25×10^4 years) and it emits no gamma-rays.

We investigated the possibility of AMS measurements for studying this reaction. No AMS measurements exists so far for ²⁰²Pb. Experience on the performance at VERA for heavy isotopes

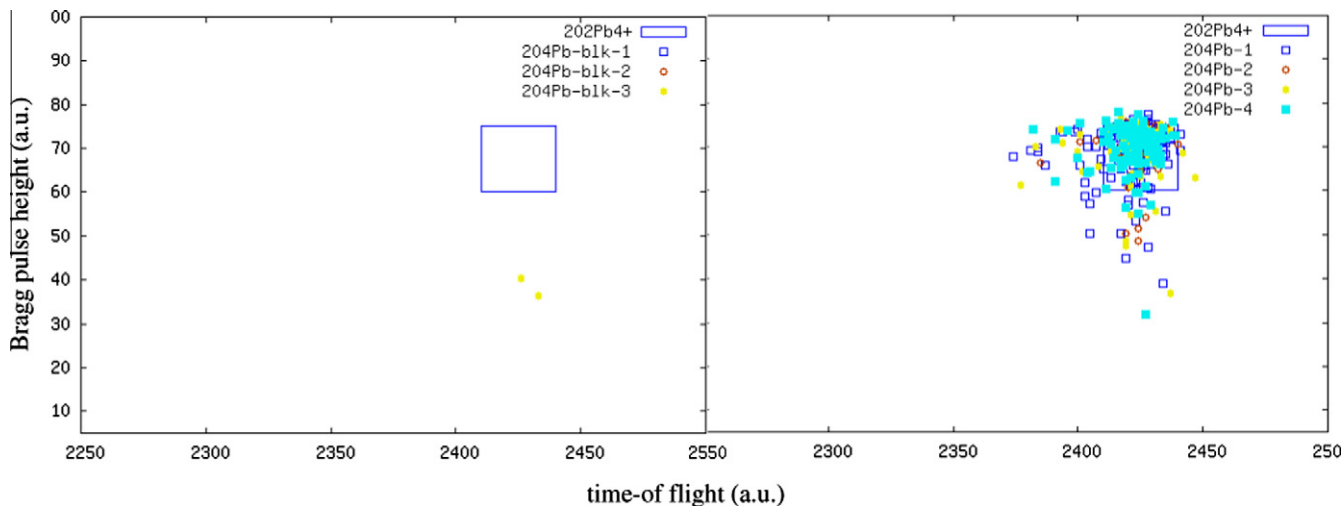


Fig. 5. Time-of-flight and energy spectra measured at VERA for Pb samples highly enriched in ^{204}Pb . The left plot shows results for un-irradiated (blank) samples. The right plot shows the signals obtained from 4 neutron-irradiated samples. The (blue) rectangle indicates the region of interest for ^{202}Pb detection. (For interpretation of the references to color in this figure legend, the reader is referred to the web version of this article.)

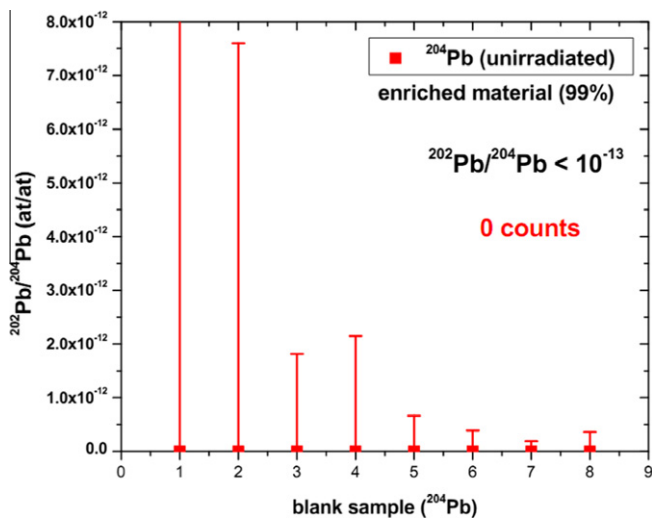


Fig. 6. AMS measurements at VERA for enriched ^{204}Pb samples. Non-irradiated blank samples were analyzed in three beam times. No detector count was registered for ^{202}Pb , corresponding to an upper limit $<10^{-13}$ for $^{202}\text{Pb}/^{204}\text{Pb}$ (statistics according to [20]).

has shown that isotope ratios $^{202}\text{Pb}/^{204}\text{Pb}$ of several 10^{-12} need to be produced in neutron irradiations in order to obtain good quantitative results. As mentioned above, in case of ^{202}Pb no interference from lower masses was expected.

Lead samples, highly enriched in ^{204}Pb , were activated with neutrons at IRMM with neutron energies of 18 and 20.5 MeV. We estimated the following numbers: assuming a cross-section value of 0.25 barn (at 18 MeV) and 1 barn (at 20.5 MeV), and a neutron flux of $2 \times 10^7 \text{ s}^{-1}$, conversion ratios $^{202g}\text{Pb}/^{204}\text{Pb}$ of 2.5×10^{-12} and 1×10^{-11} were calculated for 100 h continuous neutron irradiation.

Table 2

Summary of AMS performance for ^{55}Fe , ^{68}Ge and ^{202g}Pb at VERA. ^{202g}Pb was measured relative to ^{208}Pb and to enriched ^{204}Pb . Background ratios means the measured isotope ratio of radionuclide and reference isotope for natural (un-irradiated) and unprocessed material.

Radionuclide	Neg. ion	Reference isotope	Max. ion current	Detector	Background ratios
^{55}Fe	Fe^-	^{56}Fe	1.5 μA	Ion. chamb.	$<10^{-15}$
^{68}Ge	Ge^-	^{70}Ge	5 μA	Ion. chamb.	$<2 \times 10^{-16}$
^{202g}Pb	Pb^-	^{208}Pb	40 nA	TOF/E	$<5 \times 10^{-14}$

The isotope ratio $^{202}\text{Pb}/^{204}\text{Pb}$ produced in the neutron irradiation was measured at VERA and normalized to the $^{202}\text{Tl}/^{203}\text{Tl}$ ratios of the parallel measured Tl reference samples (see above). Typical spectra for enriched ^{204}Pb samples are shown in Fig. 5. Plotted are energy versus time-of-flight (TOF) spectra for three blank samples (Pb foils, highly enriched in ^{204}Pb , not irradiated) and for four sputter cathodes of a neutron irradiated ^{204}Pb sample (right plot). The region of interest in energy and TOF for $^{202}\text{Pb}^{4+}$ signals is indicated by the rectangle. No events were registered for non-irradiated samples during any of the beam times (see Fig. 6) which confirms the low background results for AMS measurements on ^{nat}Pb samples (see above). The irradiated samples show clear ^{202}Pb signals. Isotope ratios $^{202g}\text{Pb}/^{204}\text{Pb}$ of 6×10^{-12} and 1.4×10^{-11} were measured for samples irradiated with neutrons with energies of 18 and 20.5 MeV, respectively, i.e. isotope ratios more than two orders of magnitude above background. The final uncertainty in the cross-section data will be dominated by the uncertainty in the isotope ratio of the reference material.

5. Summary

AMS offers highest sensitivity for radionuclides which can be measured isobar-free. Besides the well-known cases of ^{14}C , ^{26}Al , ^{129}I or molecules like $^{41}\text{CaH}_3$ and the actinides, a few additional isotopes belong to the same category: ^{55}Fe , ^{68}Ge and ^{202g}Pb can be measured isobar-free as well, because manganese, zinc and mercury do not form stable negative ions. ^{55}Fe is sandwiched by stable ^{54}Fe and ^{56}Fe , therefore some isotopic suppression is required, to reduce leaky $^{54}\text{FeH}^-$ in the beam. The two other isotopes, ^{68}Ge and ^{202g}Pb are both two mass units below the first stable isotope (^{70}Ge and ^{204}Pb , respectively). Moreover, their stable isobar is also two units in charge lower. Thus, natural production is expected to be low. AMS measurements at VERA for these radionuclides indeed showed no measurable contents of these

radionuclides in natural samples. Isotope ratios of $<10^{-15}$, $\approx 10^{-16}$ and $\approx 2 \times 10^{-14}$ were measured in blank samples for $^{55}\text{Fe}/^{56}\text{Fe}$, $^{68}\text{Ge}/^{70}\text{Ge}$ and $^{202}\text{Pb}/\text{Pb}$, respectively (see Table 2). The low background of ^{68}Ge -AMS was independently confirmed at ANSTO. The few events registered in ^{68}Ge measurements at VERA might be attributed to cross-talk from reference materials in the MC SNICS ion source which may occur at levels of 10^{-4} to 10^{-5} relative to the reference samples.

Such a high sensitivity in AMS detection opens interesting applications, e.g. in nuclear astrophysics, fundamental physics studies or in technological applications. These non-standard AMS isotopes, however, require the production of appropriate reference samples. For ^{55}Fe , several grams of a new reference material with an accuracy of $\pm 1.6\%$ were produced via dilution of a precisely known ^{55}Fe reference solution. In case of ^{68}Ge and ^{202}Pb , reference samples were produced by intense sample irradiations with fast neutrons and subsequent measurement of the activity of their shorter-lived decay products, ^{68}Ga and ^{202}Tl , respectively, which were in radioactive equilibrium with their parents. In addition, neutron irradiation of ^{203}Tl produced directly ^{202}Tl which served as a proxy for ^{202}Pb measurements.

Acknowledgements

Part of this work was funded by the Austrian Science Fund (FWF): project numbers AP20434 and AI00428. Part of this work was also funded by the European EUFRAT programme.

References

- [1] H. Junde, Data Sheets for $A = 55$, Nucl. Data Sheets 109 (2008) 787; H. Schoetzig, Half-life and X-ray emission probabilities of ^{55}Fe , Appl. Rad. Isotopes 53 (2000) 469.
- [2] Decay data evaluation project, <http://www.nucleide.org/DDEP_WG/DDEPdata.htm> (2008).
- [3] H. Nagai, O. Nitoh, M. Honda, Half-life of ^{202}Pb , Radiochim. Acta 29 (1981) 169.
- [4] G. Korschinek, D. Mueller, T. Faestermann, A. Gillitzer, E. Nolte, M. Paul, Trace Analysis of ^{55}Fe in biosphere and technology by means of AMS, Nucl. Instr. Meth. B52 (1990) 498–503.
- [5] A. Wallner et al., Precise measurement of the neutron capture reaction $^{54}\text{Fe}(n, \gamma)^{55}\text{Fe}$ via AMS, J. Phys. Conf. Series 202 (2010) 012020.
- [6] A. Wallner, K. Buczak, T. Faestermann, A. Klix, G. Korschinek, C. Lederer, A. Plompen, M. Poutivstev, G. Rugel, K. Seidel, V. Semkova, H. Vonach, Production of long-lived radionuclides ^{10}Be , ^{14}C , ^{53}Mn , ^{55}Fe , ^{59}Ni and ^{202}Pb in a fusion environment, J. Korean Phys. Soc. 59 (2011) 1378.
- [7] T. Andersen, H.K. Haugen, H. Hotop, Binding energies in atomic negative ions: III, J. Phys. Chem. Ref. Data 28 (1999) 1511.
- [8] A. Fessler, S.M. Qaim, Radiochim. Acta 84 (1999) 1–10.
- [9] K. Kossert, A. Grau Carles, The LSC efficiency for low-Z electron-capture nuclides, Appl. Radiat. Isot. 64 (2006) 1446–1453.
- [10] A. Wallner, M. Bichler, I. Dillmann, R. Golser, F. Käppeler, W. Kutschera, M. Paul, A. Priller, P. Steier, C. Vockenhuber, AMS measurements of ^{41}Ca and ^{55}Fe at VERA – two radionuclides of astrophysical interest”, Nucl. Instr. Meth. B259 (2007) 677.
- [11] <http://www.ptb.de/en/org/6/61/611/katalog/allgemeines_en.htm>.
- [12] J. Magill, G. Pfennig, J. Galy, Karlsruhe Nuklidkarte, seventh ed., 2006, Revised printing, November 2009.
- [13] A. Wallner, Nuclear astrophysics and AMS – probing nucleosynthesis in the lab, Nucl. Instr. Meth. B 268 (2010) 1277.
- [14] A. Wallner, K. Buczak, I. Dillmann, J. Feige, F. Käppeler, G. Korschinek, C. Lederer, A. Mengoni, U. Ott, M. Paul, G. Schätzel, P. Steier, H.P. Trautvetter, AMS applications in nuclear astrophysics – new results for $^{13}\text{C}(n, \gamma)^{14}\text{C}$ and $^{14}\text{N}(n, p)^{14}\text{C}$, Publ. Astron. Soc. Aust. (PASA) (2012) AS11069, <http://dx.doi.org/10.1071/AS11069>.
- [15] M.B. Chadwick et al., ENDF/B-VII.1 nuclear data for science and technology: cross sections, covariances, fission product yields and decay data, Nucl. Data Sheets 112 (2011) 2887–2996.
- [16] K. Seidel et al., Fusion Eng. Des. 81 (2006) 1211.
- [17] V. Semkova et al., Phys. Rev. C80 (2009) 02461.
- [18] E. Zimmermann, J.T. Cessna, R. Fitzgerald, J. Res. Natl. Inst. Stand. Technol. 113 (2008) 265.
- [19] E. Schönfeld, U. Schötzgig, E. Günther, H. Schrader, Appl. Rad. Isot. 45 (1994) 955.
- [20] Roy Middleton, A Negative-Ion Cookbook, unpublished, October 1989 (Revised February 1990), see <<http://www.pelletron.com/cookbook.pdf>>.
- [21] O. Forstner, L. Michlmayr, M. Auer, R. Golser, W. Kutschera, A. Priller, P. Steier, A. Wallner, Applications of a compact ionization chamber in AMS at energies below 1 MeV/amu, Nucl. Instr. Meth. B 266 (2008) 2213.
- [22] G.J. Feldman, R.D. Cousins, Unified approach to the classical statistical analysis of small signals, Phys. Rev. D 57 (1998) 3873–3889.
- [23] W. Wagner, J. Mesot, P. Allenspach, G. Kuehne, H.M. Rønnow, The Swiss spallation neutron source SINQ – developments and upgrades for optimized user service, Phys. B 385–386 (2006) 968.
- [24] M.A.C. Hotchkis, D. Child, D. Fink, G.E. Jacobsen, P.J. Lee, N. Mino, A.M. Smith, C. Tuniz, Measurement of ^{236}U in environmental media, Nucl. Instr. Meth. B 172 (2000) 659.
- [25] Y. Amelin, W.J. Davis, Isotopic analysis of lead in sub-nanogram quantities by TIMS using a ^{202}Pb – ^{205}Pb spike, J. Anal. At. Spectrom. 21 (2006) 1053.
- [26] W. Henning, D. Schüll, On isobar separation and accelerator mass spectrometry of ^{205}Pb , NIM A 271 (1988) 324–327.
- [27] X.-L. Zhao, M.-J. Nadeau, L.R. Kilius, A.E. Litherland, The first detection of naturally-occurring ^{236}U with accelerator mass spectrometry, NIM B92 (1994) 249.
- [28] D. Berkovits, H. Feldstein, S. Ghelberg, A. Hershkovitz, E. Navon, M. Paul, ^{236}U in uranium minerals and standards, NIM B 172 (2000) 372.
- [29] P. Steier et al., Analysis and application of heavy isotopes in the environment, Nucl. Instr. Meth. B 268 (2010) 1045.
- [30] L.K. Fifield, S. Tims, T. Fujioka, W. Hoo, S. Everett, Accelerator mass spectrometry with the 14UD accelerator at the Australian National University, NIM B 268 (2010) 858.
- [31] A. Wallner, T. Belgya, M. Bichler, K. Buczak, I. Dillmann, F. Käppeler, A. Mengoni, F. Quinto, P. Steier, L. Szentmiklosi, Neutron capture studies on ^{235}U and ^{238}U via AMS, J. Korean Phys. Soc. 59 (2011) 1410.
- [32] P. Steier, R. Golser, W. Kutschera, A. Priller, C. Vockenhuber, A. Wallner, S. Winkler, Opportunities and limits of AMS with 3-MV tandem accelerators, Nucl. Instr. Meth. B240 (2005) 445.
- [33] S. Leray, A. Boudard, J.C. David, L. Donadille, C. Villagrasa, C. Volant, Impact of high-energy nuclear data on radioprotection in spallation sources, Radiat. Prot. Dosim. 115 (2005) 242.